| | |
|---|---|
| Title | Parametric quadratic programming method for elastic contact fracture analysis |
| Author(s) | Su, RKL; Zhu, Y; Leung, AYT |
| Citation | International Journal Of Fracture, 2002, v. 117 n. 2, p. 143-157 |
| Issued Date | 2002 |
| URL | http://hdl.handle.net/10722/48536 |
| Rights | The original publication is available at www.springerlink.com |

*Submitted to International Journal of Fracture in July 2001, revised in June 2002*

# PARAMETRIC QUADRATIC PROGRAMMING METHOD FOR ELASTIC CONTACT FRACTURE ANALYSIS

R. K. L. SU[1,a] Y. ZHU[2]

A.Y.T. Leung[3]

[1] Department of Civil Engineering, The University of Hong Kong, Pokfulam Road, Hong Kong, P.R.China

[2] Department of Civil Engineering, The University of Hong Kong, Pokfulam Road, Hong Kong, P.R.China

[3] Department of Building and Construction, City University of Hong Kong, Tat Chee Avenue, Kowloon, Hong Kong, P.R.China

[a] Corresponding Author: Fax (852) 2559 5337
Email: klsu@hkucc.hku.hk

**Total Number of Pages: 25**

**Number of Figures: 7**

**Abstract.** A solution procedure for elastic contact fracture mechanics has been proposed in this paper. The procedure is based on the quadratic programming and finite element method (FEM). In this paper, parametric quadratic programming method for two-dimensional contact mechanics analysis is applied to the crack problems involving the crack surfaces in frictional contact. Based on a linear complementary contact condition, the parametric variational principle and FEM, a linear complementary method is extended to analyze contact fracture mechanics. The near-tip fields are properly modeled in the analysis using special crack tip elements with quarter-point nodes. Stress intensity factor solutions are presented for some frictional contact fracture problems and are compared with known results where available.

Keywords: Quadratic programming, frictional contact, stress intensity factors, finite element method

## 1. Introduction

Problems in contact fracture mechanics about brittle material are very popular in practical engineering. Concrete and rocks are mainly subject to compressive loads, when external loadings are applied, contact between the crack surfaces may occur and will affect the fracture behaviors. The efficient numerical technique which can estimate the influence of the contact behaviors of the crack surfaces on the stress intensity factors of contact crack is, thus, imperative.

Within the assumption of the linear elastic model for the materials, contact frictional crack is a typical nonlinear problem as the boundary conditions of both the location and the extension of the contact zone are unknown and are depended on the applied load. This problem has received much attention over the years by many authors with different approaches. Analytical methods are particularly attractive as general and accurate solutions could be obtained, but an explicit analytical solution for contact fracture mechanics has yet to be obtained. For these reasons many researchers presented different approximate analytical solutions of some particular examples for illustrating their proposed methods. Bowie and Freese(1976) proposed to correct certain crack solutions that yield overlapping of the crack faces by introducing closure without slip in a segment of the crack. Their solutions are expected to be applicable for relatively large values of the coefficient of friction. Comninou and Dundurs(1979) extended the Bowie-Freese analysis to include the effect of friction by using a singular integral equation approach. Melville(1977) got the analytical formulations by assuming that the whole contact crack surfaces slip along each other under compressive loading based on Coulomb's frictional law. Woo *et al.* (1988) used a boundary collocation method to calculate the length of the closed part of the crack and the stress intensity factor (SIF) value of the other crack tip. Beghini and Bertini(1996) applied weight function (WF) method to the problem of a crack in bending for which the integrations could be performed analytically, the SIF and the contact stress could be obtained effectively. Numerical solutions obtained either by the finite element(FE) or the boundary element(BE) method can be found in literatures. Fredriksson(1976) presented a FE solution of contact fracture mechanics. Thiagarajan and

Alwar(1986) applied superelement technique to study the crack closure phenomena in the case of an inclined crack. Cords and Joseeph(1994) used the line spring model to iteratively determine the border of the closed portion of the crack and the SIFs along the open portion. Liu and Tan(1992) and Chen and Chen(1998) used BE methods to solve crack problems involving crack surfaces in contact. Those numerical solutions require iterative procedures which can be automatically controlled by the program, however, the contact status (stick, slip or separation) has to be repeatedly adjusted with a heuristic trial-and-error manner until the real contact status is found.

Leung *et al.* (1998) proposed smoothing Newton method for solving two- and three-dimensional frictional contact problems. In the present paper, parametric quadratic programming method for two-dimensional contact mechanics (Zhong and Sun, 1989, Klarbring, 1986), is extended to solve the crack problems involving crack surfaces in frictional contact. It has been noticed that many methods proposed to deal with frictional contact problems adopted iterative trial-and-error methods (Chan and Tuba, 1971, Okamoto and Nakazawa, 1979), however, quadratic programming method offers an effective alternative for the manipulation of contact interface inequalities and has been extensively used for the solution of contact problems using the finite FE method. The prime advantage of this technique over the iterative trial-and-error method lies in the fact that it does not involve a constant tracking of the individual nodes for contact and release. For plane elastic contact problems, iteration is unnecessary, only one step arrives the solution in the FE method sense. This method, however, has not been received much attention in the field of contact fracture mechanics. In this paper, a linear complementary contact condition (contact state equations) by Zhong and Sun, 1989 together with the parametric variational principle and FE techniques is used to solve the contact fracture problems. A quadratic programming method for elastic contact fracture problems with friction is proposal. This method can avoid the tiresome iteration procedure used in previous work, and if there is no unloading, only one incremental step is sufficient for getting the solution. The near-tip fields are properly modeled in the analysis using special crack tip elements with quarter-point nodes (Barsoum, 1976). Stress intensity factor solutions are presented for some frictional contact fracture problems and are compared

with known results where available.

## 2. Parametric quadratic programming method for elastic contact analysis

The present analysis of contact fracture mechanics considers only the static two-dimensional elasticity with small deformations. Based on these assumptions, the contact surface may be considered to be a series of points where each point is interpreted as a node on each surface. Although in this paper, the contact fracture system consists of single crack only in a linear elastic body, the discussions can be easily extended to the problems involved multiple cracks.

### 2.1. The description of contact problems and contact constitutive model

Consider the contact system consisting of a linear elastic body occupying an open set Ω which is defined in the global co-ordinate system (*o-xy*). The possible contact faces of the crack in the body are $s^1$ and $s^2$. The gap $\delta^*$ between the contact faces is very small so $s^c$ used to express the common possible contact boundary ($s^1$ and $s^2$), as shown in Figure 1.

Contact problem is an inherently nonlinear and irreversible problem. It is subjected to the unilateral constraints and the contact faces must not penetrate each other. The contact conditions between the two faces are described by Coulomb's law, so that the contact and slippery conditions (Zhong and Sun, 1989) can be expressed as:

$$\widetilde{f}_1 = p_\tau + \overline{\mu} p_n \le 0 \tag{1}$$

$$\widetilde{f}_2 = -p_\tau + \overline{\mu} p_n \le 0 \tag{2}$$

$$\widetilde{f}_3 = p_n \le 0 \tag{3}$$

where $\widetilde{f}_k$ (k=1,2,3) are called the *contact and slip functions*, $p_\tau$ and $p_n$ are tangential and normal stresses in a local coordinate system ($o'$-$n\,\tau$) of the candidate contact point with

respect to crack surfaces. Here, $n^{(i)}$ and $\tau^{(i)}$ denote the unit outward normal boundary vector and the tangential boundary vector of crack surface $s^{(i)}$. In particularly, take the nodes on surface '2' as master, on surface '1' as slave and the vectors $n=n^{(2)}$, $\tau=\tau^{(2)}$ as the local system. $\overline{\mu}$ is Coulomb's frictional coefficient. Different values of $f_k$ associate with different contact conditions. For example, when $\widetilde{f}_1=0$ or $\widetilde{f}_2=0$, contact slip occurs along positive or negative tangential directions, respectively, when $\widetilde{f}_1<0$ or $\widetilde{f}_2<0$ there is no slip, when $\widetilde{f}_3=0$, separation occurs along normal direction.

The relative displacements in tangential and normal directions of any pair of candidate contact points are defined as,

$$\boldsymbol{\varepsilon}_c=\{\varepsilon_\tau,\varepsilon_n\}^T \tag{4}$$

where
$$\begin{cases}\varepsilon_\tau=u_\tau^1-u_\tau^2=\Delta u_\tau\\ \varepsilon_n=u_n^1-u_n^2+\delta^*=\Delta u_n+\delta^*\end{cases} \tag{5}$$

$\boldsymbol{\varepsilon}_c$ is the relative displacements of candidate contact pair points**.** In this paper capital boldface letters are used to denote matrices, lowercase boldface letters denote vectors and lowercase letters denote the components of corresponding vectors. $u_\tau^i$ and $u_n^i$ are the tangential and normal nodal displacements respectively, at an arbitrary candidate contact point with respect to crack surface $s^i$, ($i$=1,2). $\delta^*$ is the normal initial gap between the potential contact points.

The general case of elastic contact problems with Coulomb's friction law is characterized by the following system of equations and inequalities:

$$\varepsilon_n\ge 0,\ p_n\le 0\ ,\ \varepsilon_n.p_n=0 \tag{6}$$

$$\varepsilon_\tau=0\quad \text{when}\ \ |p_\tau|\le-\overline{\mu}p_n \tag{7}$$

$$|\varepsilon_\tau|\ge 0\quad \text{when}\ |p_\tau|=-\overline{\mu}p_n \tag{8}$$

By the rigid elasticity model that is an analogy from plasticity flow theory, we can express $p_\tau$ and $p_n$ in terms of relative displacements by equations (6) to (8) as below:

$$\begin{aligned} p_n &= E_n \cdot \beta(\varepsilon_n) \\ \beta(\varepsilon_n) &= \varepsilon_n \cdot [1 - sign(\varepsilon_n)]/2 \end{aligned} \tag{9}$$

$$p_\tau = \begin{cases} E_\tau \cdot \varepsilon_\tau, & |p_\tau| < -\bar{\mu} p_n \\ -\bar{\mu} p_n sign(\varepsilon_\tau), & |p_\tau| = -\bar{\mu} p_n \end{cases} \tag{10}$$

where sign(*) equal –1 when *<0 or 1 when $* \geq 0$, $E_n$ and $E_\tau$ are the penalty factors. It is obviously that the relative displacement vector can be expressed as:

$$\boldsymbol{\varepsilon}_c = \boldsymbol{\varepsilon}_c^e + \boldsymbol{\varepsilon}_c^p \tag{11}$$

where $\boldsymbol{\varepsilon}_c^e$ is contact elastic relative displacement vector and $\boldsymbol{\varepsilon}_c^p$ is contact slip relative displacement vector. Denoting the contact stress vector to be $\mathbf{p}_c$ so that

$$\mathbf{p}_c = \{p_\tau \quad p_n\}^T \tag{12}$$

by substituting equations (9) to (11) into equation (12), we can have

$$\mathbf{p}_c = \mathbf{D}_c \boldsymbol{\varepsilon}_c^{\mathrm{e}} = \mathbf{D}_{\mathrm{c}} \left( \boldsymbol{\varepsilon}_c - \boldsymbol{\varepsilon}_c^p \right) \tag{13}$$

where

$$\mathbf{D}_c = \begin{bmatrix} E_\tau & 0 \\ 0 & E_n \end{bmatrix} \tag{14}$$

equation (13) represents the contact constitutive relation model which is expressed in terms of the penalty functions.

2.2. The expressions of contact slip conditions by displacements (*state equations*)

By Coulomb's fractional law of equation (1), contact slippery occurs when $\widetilde{f}_k = 0$ for $k$ equal 1,2 or 3. In more details, $\widetilde{f}_1 = 0$ and $\widetilde{f}_2 = 0$ are defined as the positive and negative tangential slips with movement of $\widetilde{\lambda}_1$ and $-\widetilde{\lambda}_2$ respectively. $\widetilde{f}_3 = 0$ is equivalent to the case of normal separation with movement of $\widetilde{\lambda}_3$. It is apparent that all the values of $\widetilde{\lambda}_k$ are always greater than or equal to zero.

Using an analogy from plasticity flow theory we define the *slip potential functions* $\widetilde{g}_k$ (which are corresponding to the contact and slippery conditions $\widetilde{f}_k$) as follows:

$$\begin{cases} \widetilde{g}_1 = p_\tau + c_0 \\ \widetilde{g}_2 = -p_\tau + c_0 \\ \widetilde{g}_3 = p_n \end{cases} \tag{15}$$

Where $c_0$ is some constant. The contact slip relative displacement vector can be related with $\widetilde{\lambda}_k$ and are expressed as follows:

$$\boldsymbol{\varepsilon}_c^p = \sum_{k=1}^{3} \widetilde{\lambda}_k \cdot \left( \frac{\partial \widetilde{g}_k}{\partial \mathbf{p}_c} \right)^T \tag{16}$$

where the partial $\dfrac{\partial \widetilde{g}_k}{\partial \mathbf{p}_c}$ define the directions of slip for the displacements vector $\boldsymbol{\varepsilon}_c^p$. Equation (16) is called the *contact slip law* and can be rewritten in matrix form,

$$\boldsymbol{\varepsilon}_c^p = \left( \frac{\partial \widetilde{\mathbf{g}}}{\partial \mathbf{p}_c} \right)^T \widetilde{\boldsymbol{\lambda}} \tag{16a}$$

Where $$\widetilde{\mathbf{g}} = \begin{bmatrix} \widetilde{g}_1 & \widetilde{g}_2 & \widetilde{g}_3 \end{bmatrix}^T \tag{17}$$

$$\widetilde{\boldsymbol{\lambda}} = \begin{bmatrix} \widetilde{\lambda}_1 & \widetilde{\lambda}_2 & \widetilde{\lambda}_3 \end{bmatrix}^T \tag{18}$$

$$\frac{\partial \widetilde{\mathbf{g}}}{\partial \mathbf{p}_c} = \begin{bmatrix} \dfrac{\partial \widetilde{g}_1}{\partial p_\tau} & \dfrac{\partial \widetilde{g}_1}{\partial p_n} \\ \dfrac{\partial \widetilde{g}_2}{\partial p_\tau} & \dfrac{\partial \widetilde{g}_2}{\partial p_n} \\ \dfrac{\partial \widetilde{g}_3}{\partial p_\tau} & \dfrac{\partial \widetilde{g}_3}{\partial p_n} \end{bmatrix} \tag{19}$$

$\widetilde{f}_k < 0$ implies the case of contact adhesive and thus $\widetilde{\lambda}_k = 0$. However, when $\widetilde{f}_k = 0$ and $\widetilde{\lambda}_k > 0$ which represents the conditions of contact slippery. It is noted that $\widetilde{\lambda}_3 \geq 0$ represents the case of separation that is also considered as a kind of slippery in our study. By substituting the constitutive model of equation (13) and the contact slippery laws of equation (16a) into the expressions of $\widetilde{f}_k$ in the equation (1) to (3), we have,

$$\widetilde{f}_1 = E_\tau \Delta u_\tau + \overline{\mu} E_n \left(\Delta u_n + \delta^*\right) - E_\tau \widetilde{\lambda}_1 \leq 0 \tag{20}$$

$$\widetilde{f}_2 = -E_\tau \Delta u_\tau + \overline{\mu} E_n \left(\Delta u_n + \delta^*\right) - E_\tau \widetilde{\lambda}_2 \leq 0 \tag{21}$$

$$\widetilde{f}_3 = E_n \left(\Delta u_n + \delta^*\right) - E_n \widetilde{\lambda}_3 \leq 0 \tag{22}$$

By introducing the constraint relax variables $\widetilde{\upsilon}_k$, let

$$\widetilde{f}_k \left(\Delta u_\tau, \Delta u_n, \widetilde{\lambda}_k\right) + \widetilde{\upsilon}_k = 0, \; k=1,2,3. \tag{23}$$

When equation (23) subjected to the conditions of contact adhesive and contact slippery (their corresponding mathematical expressions are $\widetilde{\lambda}_k = 0$ and $\widetilde{f}_k < 0$; and $\widetilde{\lambda}_k > 0$ and $\widetilde{f}_k = 0$ respectively), we can show that $\widetilde{\lambda}_k \cdot \widetilde{\upsilon}_k = 0,$ where $\widetilde{\lambda}_k, \widetilde{\upsilon}_k \geq 0,$ and $k = 1,2,3$. Hence equation(23) can be expressed in the following matrix form,

$$\begin{aligned} &\widetilde{\mathbf{f}}\left(\mathbf{u}_c, \widetilde{\boldsymbol{\lambda}}\right) + \widetilde{\boldsymbol{\upsilon}} = \mathbf{0} \\ &\widetilde{\boldsymbol{\upsilon}}^T \cdot \widetilde{\boldsymbol{\lambda}} = \mathbf{0}, \quad \widetilde{\boldsymbol{\upsilon}}, \widetilde{\boldsymbol{\lambda}} \geq \mathbf{0} \end{aligned} \tag{24}$$

where $\widetilde{\mathbf{f}} = \begin{pmatrix} \widetilde{f}_1 & \widetilde{f}_2 & \widetilde{f}_3 \end{pmatrix}^T$ (25)

$$\widetilde{\mathbf{u}}_c = \begin{pmatrix} \Delta u_\tau & \Delta u_n \end{pmatrix}^T \tag{26}$$

$$\widetilde{\boldsymbol{\upsilon}} = \begin{pmatrix} \widetilde{\upsilon}_1 & \widetilde{\upsilon}_2 & \widetilde{\upsilon}_3 \end{pmatrix}^T \tag{27}$$

$$\widetilde{\boldsymbol{\lambda}} = \begin{pmatrix} \widetilde{\lambda}_1 & \widetilde{\lambda}_2 & \widetilde{\lambda}_3 \end{pmatrix}^T \tag{28}$$

Equation (24) is the *contact state equation* denoting a linear complementary contact condition with contact relative displacements. In component form, the *contact state equations* can be expressed as:

$$\begin{gathered} \widetilde{f}_k^0 + \widetilde{\mathbf{w}}_k \boldsymbol{\varepsilon}_c - \widetilde{\mathbf{m}}_k \widetilde{\boldsymbol{\lambda}} + \widetilde{\upsilon}_k = 0 \\ \widetilde{\lambda}_k \cdot \widetilde{\upsilon}_k = 0, \\ \widetilde{\lambda}_k, \widetilde{\upsilon}_k \geq 0, \, k = 1,2,3 \end{gathered} \tag{29}$$

where $\widetilde{f}_k^0$ denotes the beginning value of $\widetilde{f}_k$,

$$\widetilde{\mathbf{w}}_k = \left[ \frac{\partial \widetilde{f}_k}{\partial \mathbf{p}_c} \right] \mathbf{D}_c \text{ and } \widetilde{\mathbf{m}}_k = \left[ \frac{\partial \widetilde{f}_k}{\partial \mathbf{p}_c} \right] \mathbf{D}_c \left( \frac{\partial \widetilde{\mathbf{g}}}{\partial \mathbf{p}_c} \right) \tag{30}$$

2.3. The parametric quadratic programming method of elastic contact fracture problem

The solution of the boundary value problems of plane elastic contact fracture should satisfy both the general elasticity equations and the contact state equations (24) on the contact boundary $s^c$. According to the plane elastic contact parametric variable minimum potential energy theory (Zhong and Zhang, 1997), the true displacement field corresponds to the minima of the total potential energy function (as shown below) subjected to the condition of the contact state equations (24)

$$\prod = \int_\Omega \frac{1}{2} \boldsymbol{\varepsilon}^T \mathbf{D} \boldsymbol{\varepsilon} d\Omega - \left[ \int_\Omega \mathbf{b}^T \mathbf{u} d\Omega + \int_{s_p} \overline{\mathbf{p}}^T \mathbf{u} ds \right] + \int_{s_c} \left( \frac{1}{2} \boldsymbol{\varepsilon}_c^T \mathbf{D}_c \boldsymbol{\varepsilon}_c - \widetilde{\boldsymbol{\lambda}}^T \widetilde{\mathbf{R}} \boldsymbol{\varepsilon}_c \right) ds \tag{31}$$

where $\widetilde{\mathbf{R}} = \left( \frac{\partial \widetilde{\mathbf{g}}}{\partial \mathbf{p}_c} \right) \mathbf{D}_c$ (32)

$\overline{\mathbf{p}}$ and $\mathbf{b}$ are the surface traction vector and the body force vector,respectively.

By finite element method, the whole contact fracture mechanics system is discretized into finite elements. It is noted that the candidate contact boundary of the crack faces must be

discretized and connected with contact elements. The region around the crack tip is modeled by singularity elements. The cracked body and the surface area of the body are represented by

$$\Omega = \sum_{e=1}^{N_e} \Omega_e \quad \text{and} \quad s_c = \sum_{e=1}^{N_c} s_c^e \tag{33}$$

The state equation (29) of the contact element '*e*' becomes:

$$\int_{s_c^e} \left( \tilde{f}_\alpha^{0^e} + \tilde{\mathbf{w}}_\alpha^e \boldsymbol{\varepsilon}_c^{\ e} - \tilde{\mathbf{m}}_\alpha^e \tilde{\boldsymbol{\lambda}}^e \right) ds + \tilde{\upsilon}_\alpha^e = 0 \tag{34}$$

$$\tilde{\upsilon}_\alpha^{\mathrm{e}} . \tilde{\boldsymbol{\lambda}}_\alpha^{\mathrm{e}} = 0, \quad \tilde{\upsilon}_\alpha^{\mathrm{e}}, \tilde{\boldsymbol{\lambda}}_\alpha^{\mathrm{e}} \geq 0 \tag{35}$$

where $\alpha = 1,2,3$ $e$=1,2,3,…, $N_c$. $N_c$ is the total number of contact elements. Therefore, the contact state equation of the whole system becomes:

$$\sum_{e=1}^{N_c} \left\{ \int_{s_c^e} \mathbf{T}_\lambda^{e^T} \tilde{\mathbf{f}}^{0^e} ds + \int_{s_c^e} \mathbf{T}_\lambda^{e^T} \tilde{\mathbf{w}}^e \boldsymbol{\varepsilon}_c^e ds - \int_{s_c^e} \mathbf{T}_\lambda^{e^T} \tilde{\mathbf{m}}^e \mathbf{T}_\lambda^e \tilde{\boldsymbol{\lambda}}^e ds \right\} + \tilde{\boldsymbol{\upsilon}}^e = 0 \tag{36}$$

where

$$\tilde{\mathbf{w}}^e = \left( \frac{\partial \tilde{\mathbf{f}}^e}{\partial \mathbf{p}_c^{\ e}} \right) \mathbf{D}_c \tag{37}$$

$$\tilde{\mathbf{f}}^e = \begin{bmatrix} \tilde{f}_1^e & \tilde{f}_2^e & \tilde{f}_3^e \end{bmatrix}^T \tag{38}$$

$$\tilde{\mathbf{m}}^e = \left[ \frac{\partial \tilde{\mathbf{f}}^e}{\partial \mathbf{p}_c^e} \right] \mathbf{D}_c \left[ \frac{\partial \tilde{\mathbf{g}}^e}{\partial \mathbf{p}_c^e} \right]^T \tag{39}$$

$$\boldsymbol{\varepsilon}_c^e = \mathbf{N}_c^e \left( \tilde{\mathbf{u}}_\mathbf{c}^\mathbf{e} + \boldsymbol{\delta}_c^{*e} \right) \tag{40}$$

$$\boldsymbol{\delta}_c^{*e} = \begin{pmatrix} 0 & \delta^{*e} \end{pmatrix}^T \tag{41}$$

and $\mathbf{T}_\lambda^e$ is the coordinate transformation matrix and $\mathbf{N}_c^e$ is the shape function matrix.

Substitute equations (40) and (41) into equation (36), we can have

$$\mathbf{C}\hat{\mathbf{u}} - \mathbf{U}\tilde{\boldsymbol{\lambda}} - \mathbf{d} + \tilde{\boldsymbol{\upsilon}} = \mathbf{0} \tag{42}$$

$$\tilde{\boldsymbol{\upsilon}}^{\mathbf{T}} \cdot \tilde{\boldsymbol{\lambda}} = \mathbf{0}, \quad \tilde{\boldsymbol{\upsilon}}, \tilde{\boldsymbol{\lambda}} \geq \mathbf{0} \tag{43}$$

where: $$\mathbf{C} = \sum_{e=1}^{N_c} \int_{S_c^e} \mathbf{T}_\lambda^{eT} \tilde{\mathbf{w}}^e \mathbf{N}_c^e \mathbf{T}_c^e ds \in R^{m_f \times N_u} \tag{44}$$

$$\mathbf{U} = \sum_{e=1}^{N_c} \int_{S_c^e} \mathbf{T}_\lambda^{eT} \tilde{\mathbf{m}}^e \mathbf{T}_\lambda^e ds \in R^{m_f \times m_f} \tag{45}$$

$$\mathbf{d} = \mathbf{d}_0 + \mathbf{d}_\delta \tag{46}$$

$$\mathbf{d}_0 = -\sum_{e=1}^{N_c} \int_{S_c^e} \mathbf{T}_\lambda^{eT} \tilde{\mathbf{f}}^{0^e} ds \tag{47}$$

$$\mathbf{d}_\delta = -\sum_{e=1}^{N_c} \int_{S_c^e} \mathbf{T}_\lambda^{eT} \tilde{\mathbf{w}}^e \mathbf{T}_\delta^e ds \cdot \boldsymbol{\delta}_c^* \tag{48}$$

Here $N_u$ is the total number of degree of freedoms of the system and $m_f$ is equal to $3\times N_c$.

Having established the contact state equation (42) for the discretized system, based on equation (31) the total potential energy of the contact discretized system can be expressed as:

$$\prod = \sum_{e=1}^{N_e} \left\{ \int_{\Omega_e} \frac{1}{2} \boldsymbol{\varepsilon}^{eT} \mathbf{D}^e \boldsymbol{\varepsilon}^e d\Omega - \left[ \int_{\Omega_e} \mathbf{b}^{eT} \mathbf{u}^e d\Omega + \int_{S_p^e} \overline{\mathbf{p}}^{eT} \mathbf{u}^e ds \right] \right\} - \sum_{e=1}^{N_c} \int_{S_c} \left( \frac{1}{2} \boldsymbol{\varepsilon}_c^{eT} \mathbf{D}_c^e \boldsymbol{\varepsilon}_c^e - \tilde{\boldsymbol{\lambda}}^{eT} \tilde{\mathbf{R}}^e \boldsymbol{\varepsilon}_c^e \right) ds \tag{49}$$

we can rewrite equation (49) such that,

$$\prod = \frac{1}{2} \hat{\mathbf{u}}^T \mathbf{K} \hat{\mathbf{u}} - \hat{\mathbf{u}}^T \left( \boldsymbol{\varphi} \tilde{\boldsymbol{\lambda}} + \hat{\mathbf{p}} \right) \tag{50}$$

where $$\mathbf{K} = \sum_{e=1}^{N_e} \mathbf{T}_e^{eT} \mathbf{K}_e \mathbf{T}_e^e + \sum_{e=1}^{N_c} \mathbf{T}_c^{eT} \mathbf{K}_e^c \mathbf{T}_c^e \in R^{N_u \times N_u} \tag{51}$$

$$\mathbf{K}_e = \int_{\Omega_e} \mathbf{B}^{eT} \mathbf{D}^e \mathbf{B}^e d\Omega \tag{52}$$

$$\mathbf{K}_e^c = \int_{S_c^e} \mathbf{N}_c^e \mathbf{D}_c^e \mathbf{N}_c^e ds \tag{53}$$

$$\boldsymbol{\varphi} = \sum_{e=1}^{N_c} \int_{S_c^e} \mathbf{T}_c^{eT} \mathbf{N}_c^{eT} \tilde{\mathbf{R}}^{eT} \mathbf{T}_\lambda^e ds \in R^{N_u \times m_f} \tag{54}$$

$$\hat{\mathbf{p}} = \hat{\mathbf{p}}_0 - \hat{\mathbf{p}}_\delta \tag{55}$$

$$\hat{\mathbf{p}}_0 = \sum_{e=1}^{Ne} \left\{ \int_{\Omega_e} \mathbf{T}_e^{eT} \mathbf{N}^{eT} \mathbf{b} d\Omega + \int_{S_p^e} \mathbf{T}_e^{eT} \mathbf{N}^{eT} \overline{\mathbf{p}} ds \right\} \tag{56}$$

$$\hat{\mathbf{p}}_\delta = \left[ \sum_{e=1}^{N_e} \mathbf{T}_c^{eT} \mathbf{k}_e^c \mathbf{T}_\delta^e \right] \boldsymbol{\delta}_c^* \in R^{N_u \times 1} \tag{57}$$

Hence the finite element formulation for plane elastic contact problem by parametric quadratic programming can be represented as:

$$\text{min: } \prod = \frac{1}{2} \hat{\mathbf{u}}^T \mathbf{K} \hat{\mathbf{u}} - \hat{\mathbf{u}}^T \left( \boldsymbol{\varphi} \tilde{\boldsymbol{\lambda}} + \hat{\mathbf{p}} \right) \tag{58}$$

$$\text{subject to: } \begin{array}{l} \mathbf{C}\hat{\mathbf{u}} - \mathbf{U}\tilde{\boldsymbol{\lambda}} - \mathbf{d} + \tilde{\boldsymbol{\upsilon}} = 0 \\ \tilde{\boldsymbol{\upsilon}}^T \cdot \tilde{\boldsymbol{\lambda}} = 0, \quad \tilde{\boldsymbol{\upsilon}}, \tilde{\boldsymbol{\lambda}} \geq 0 \end{array} \tag{59}$$

It is a convex programming problem, by using the Kuhn-Tucker condition (Reklaitis *et al* 1983), we can show that equations (58) and (59) can be converted into a linear complementary problem (LCP):

$$-\mathbf{K}^{-1} \boldsymbol{\varphi} \tilde{\boldsymbol{\lambda}} + \mathbf{I} \hat{\mathbf{u}} = \mathbf{K}^{-1} \hat{\mathbf{p}} \tag{60}$$

$$\begin{array}{c} \tilde{\boldsymbol{\upsilon}} - \left( \mathbf{U} - \mathbf{C}\mathbf{K}^{-1} \boldsymbol{\varphi} \right) \tilde{\boldsymbol{\lambda}} = -\mathbf{C}\mathbf{K}^{-1} \hat{\mathbf{p}}_0 + \mathbf{d}_0 + \left( \mathbf{d}_\delta + \mathbf{C}\mathbf{K}^{-1} \hat{\mathbf{p}}_\delta \right) \\ \tilde{\boldsymbol{\upsilon}}^T \cdot \tilde{\boldsymbol{\lambda}} = 0, \quad \tilde{\boldsymbol{\upsilon}}, \tilde{\boldsymbol{\lambda}} \geq 0 \end{array} \tag{61}$$

The near-tip fields are modeled in the analysis using special crack tip elements with quarter-point nodes. This enables the stress intensity factors $K_1$ and $K_2$ to be obtained directly from the nodal displacements, even with relatively coarse mesh discretization (Barsoum, 1976). It is noted that in frictional contact fracture mechanics analysis, when the crack is closed under compressive loads, $K_1$ is always zero and the normal stress at the crack tip is nonsingular.

**3. Techniques of finite element numerical calculation**

Different kinds of contact elements had been proposed, since linear-elastic static and small deformation contact fracture problems are considered in this paper, it is convenient to use point to point contact element at the candidate conforming contact faces of the crack. The shape function matrix of the contact element for the relative displacements of the candidate nodes is $\mathbf{N}_c^e = \begin{bmatrix} 1 & 0 \\ 0 & 1 \end{bmatrix}$. The point to point contact element stiffness becomes

$$\mathbf{K}_e^c = \begin{bmatrix} E_\tau & 0 \\ 0 & E_n \end{bmatrix} \tag{62}$$

Based on equation (62), equations (39), (44), (45) and (54) can be simplified to

$$\boldsymbol{\varphi}_e^c = \begin{bmatrix} E_\tau & -E_\tau & 0 \\ 0 & 0 & E_n \end{bmatrix} \tag{63}$$

$$\mathbf{C}_e^c = \begin{bmatrix} E\tau & \overline{\mu}E_n \\ -E_\tau & \overline{\mu}E_n \\ 0 & E_n \end{bmatrix} \tag{64}$$

$$\tilde{\mathbf{m}}^e = \mathbf{U}_e^c = \begin{bmatrix} E_\tau & -E_\tau & \overline{\mu}E_n \\ -E_\tau & E_\tau & \overline{\mu}E_n \\ 0 & 0 & E_n \end{bmatrix} \tag{65}$$

Using the matrix transformation property, equations (48) and (57) can be expressed as:

$$\mathbf{d}_\delta = -\mathbf{U}\boldsymbol{\delta}_c^* \tag{66}$$

$$\hat{\mathbf{p}}_\delta = \boldsymbol{\varphi}\boldsymbol{\delta}_c^* \tag{67}$$

It is noted that $\boldsymbol{\delta}_c^*$ corresponds to the vector space of $\tilde{\boldsymbol{\lambda}}$. Substituting equations (66) and (67) into equation (61), we can get

$$\begin{gathered} \tilde{\boldsymbol{\upsilon}} - \left(\mathbf{U} - \mathbf{C}\mathbf{K}^{-1}\boldsymbol{\varphi}\right)\tilde{\boldsymbol{\lambda}} = -\mathbf{C}\mathbf{K}^{-1}\hat{\mathbf{p}}_0 + \mathbf{d}_0 - (\mathbf{U} - \mathbf{C}\mathbf{K}^{-1}\boldsymbol{\varphi}\ )\boldsymbol{\delta}_c^* \\ \tilde{\boldsymbol{\upsilon}}^T \cdot \tilde{\boldsymbol{\lambda}} = \mathbf{0}, \quad \tilde{\boldsymbol{\upsilon}}, \tilde{\boldsymbol{\lambda}} \geq \mathbf{0} \end{gathered} \tag{68}$$

If we directly replace the penalty factors $E_\tau$ and $E_n$ with large numbers and solve equations (60) and (68), serious numerical error will be produced due to ill conditioning. By algebraically transformation, and denoting $\hat{\mathbf{u}}_s$ as the total general nodal displacements vector, $\hat{\mathbf{u}}_c$ as the total contact nodal relative displacements vector and $\boldsymbol{\delta}_c^*$ as the total contact nodal initial gap corresponding to the vector space of $\tilde{\mathbf{u}}_c$, we can eliminate the penalty factors in the equations (60) and (68) such that,

$$\begin{aligned} \mathbf{K}_{11}\hat{\mathbf{u}}_s &= \hat{\mathbf{p}}_{01} + \mathbf{K}_{12}\boldsymbol{\varphi}'(\boldsymbol{\delta}^* - \tilde{\boldsymbol{\lambda}}) \\ \hat{\mathbf{u}}_c &= -\mathbf{I}\boldsymbol{\varphi}'(\boldsymbol{\delta}^* - \tilde{\boldsymbol{\lambda}}) \end{aligned} \tag{69}$$

$$\begin{aligned} \tilde{\boldsymbol{\upsilon}} - \left(\mathbf{C}'\mathbf{K}_r\boldsymbol{\varphi}'\right)\tilde{\boldsymbol{\lambda}} &= -\mathbf{C}'\hat{\mathbf{p}}_{0r} - \left(\mathbf{C}'\mathbf{K}_r\right)\boldsymbol{\delta}_c^* + \mathbf{d}_0 \\ \tilde{\boldsymbol{\upsilon}}^T \cdot \tilde{\boldsymbol{\lambda}} = 0, \quad \tilde{\boldsymbol{\upsilon}}, \tilde{\boldsymbol{\lambda}} &\geq 0 \end{aligned} \tag{70}$$

where

$$\mathbf{C}' = \begin{bmatrix} \mathbf{C}_1' & & & \\ & \mathbf{C}_2' & & \\ & & \ddots & \\ & & & \mathbf{C}_{N_c}' \end{bmatrix} \qquad \mathbf{C}_e' = \begin{bmatrix} 1 & \bar{\mu} \\ -1 & \bar{\mu} \\ 0 & 1 \end{bmatrix} \tag{71}$$

$$\boldsymbol{\varphi}' = \begin{bmatrix} \boldsymbol{\varphi}_1' & & & \\ & \boldsymbol{\varphi}_2' & & \\ & & \ddots & \\ & & & \boldsymbol{\varphi}_{N_c}' \end{bmatrix} \qquad \boldsymbol{\varphi}_e' = \begin{bmatrix} 1 & -1 & 0 \\ 0 & 0 & 1 \end{bmatrix} \tag{72}$$

$$\hat{\mathbf{p}}_{0r} = \hat{\mathbf{p}}_{02}^c - \mathbf{K}_{21}\mathbf{K}_{11}^{-1}\hat{\mathbf{p}}_{01} \tag{73}$$

$$\hat{\mathbf{p}}_0 = \begin{Bmatrix} \hat{\mathbf{p}}_{01} \\ \hat{\mathbf{p}}_{02}^c \end{Bmatrix} \tag{74}$$

$$\mathbf{K}_r = \mathbf{K}_{22} - \mathbf{K}_{21}\mathbf{K}_{11}^{-1}\mathbf{K}_{12} \tag{75}$$

The sub-matrices $\mathbf{K}_{ij}$ can be determined by

$$\mathbf{K} = \begin{bmatrix} \mathbf{K}_{11} & \mathbf{K}_{12} \\ \mathbf{K}_{21} & \mathbf{K}_{22} + E\mathbf{K}_{22}^{c} \end{bmatrix} \tag{76}$$

where $E=E_n=E_\tau$ is penalty factor.

The equation (70) can be solved by Lemke Method (Lemke,1965). By using equation(69), we can get $\hat{\mathbf{u}}_c$ and $\hat{\mathbf{u}}_s$, and hence evaluate the SIFs.

## 4. Numerical examples

The computer program developed on the basis of the proposed method was applied to the determination of SIFs. The first example is simple crack subjected to tensile traction, although it has no contact under applied loading, it can be considered that candidate contact faces of crack is normal separation and we can use this example to test the reliability of the theory. Other examples with various contact conditions are also analysis and the results are compared with the available results.

### 4.1 *Example 1 (Central crack under tension)*

A rectangular strip with a central crack subjected to uniform tensile traction $q$=10 MPa is shown in Figure 2. The length of crack is 2$a$ perpendicular to the direction of loading. The width and the length are 2$W$ and 2$L$ respectively. Since the analytical solution available pertains to infinite lengths, 2L was assumed to be 5W so as to simulate this boundary condition. The following material properties are assumed for analysis (i) elastic module E =524.94MPa, (ii) Poisson's ratio $\upsilon$=0.3 and (iii) 2$a$=4 unit, 2$w$=20 unit. It is noted that the SIFs obtained are independent of the chosen material properties. On the possible contact surface, the results show that the tangential contact displacements are zero which agree well with the actual displacement condition. The stress intensity factor $K_1$ determined by the present method is 2390N/cm$^{3/2}$ which differs from the solution (Murakami, 1987) of $K_1$ =2510 N/cm$^{3/2}$ by 4.8%. This inaccuracy is mainly due to the deficiency of the collapsed quarter-point isoparametric elements employed in modeling the singularity at the crack tip. Similar level of inaccuracy was reported by Barsoum (1976) and Owen & Fawkes (1983) in calculating the SIFs using the same element.

4.2 Example 2 (Edge crack under bending)

A rectangular plate with an angled edge crack of length $a$ under bending moment $M$ is shown in Figure 3. The corresponding finite element mesh with six-node triangular isoparametric elements is shown in Figure 4. This problem has been studied by Liu and Tan(1992). The geometry is taken as: $L/W$=4, $a/W$=0.6, 0.8, and $\theta$=0$^o$, 45$^o$. When bending moment is applied and $\theta$=0$^o$, the crack tip only has $K_1$. The normalized mode I stress intensity factors $K_1^n=K_1/(6M\sqrt{\pi a}/W^2)$ versus various friction coefficients $\bar{\mu}$=0.0, 0.2, 0.4, 0.6 for $a/W$=0.6 and 0.8 are shown in Figure 5. When $\theta$=45$^o$ and $a/W$=0.6, under the bending moment, the whole crack surface is closed. The crack tip only has $K_2$, the normalized mode II stress intensity factors $K_2^n=K_2/(6M\sqrt{\pi a}/W^2)$ versus various friction coefficients are shown in Figure 6. When $\theta$=45$^o$ and $a/W$=0.8, under the bending moment, the crack tip has both $K_1$ and $K_2$. The normalized mode II and Mode I stress intensity factors $K_2^n$ and $K_1^n$ versus various friction coefficients are shown in Figure 6 and Figure 7 respectively. Good agreement between the present computed results and referenced solutions is also found.

## 5. Conclusions

Parametric quadratic programming contact method was presented for the determined of SIFs with crack surfaces involving frictional contact each other. The near-tip fields are properly modeled in the analysis using special crack tip elements with quarter-point nodes. These methods avoid iterative calculation and can easily be incorporated in general finite element program. The numerical examples have been given to demonstrate the accuracy and efficiency of the present method.

## 6. Acknowledgement

The work described in this paper was fully supported by the grant from the Research Grants Council of the Hong Kong Special Administrative Region, China (Project No. HKU 7014/00E).

**Reference**

Barsoum, R.S.(1976). On the use of isoparametric finites in linear fracture mechanics. *International Journal of Numerical Methods in Engineering* **10**(1) ,25-37.

Beghini, M. and Bertini, L.(1996). Effective stress intensity factor and contact stress for a partially closed Griffith crack in bending . *Engineering Fracture Mechanics* **54**, 667-678.

Bowie, O.L. and Freese, C.E.(1976). On the 'overlapping' problem in crack analysis. *Engineering Fracture Mechanics* **8**, 373-379.

Chan, S.K. and Tuba, I.S.(1971). A finite element method for contact problems of solid bodies. *International Journal of Mechanical Sciences* **13**, 615-639.

Comminu, M.and Dundurs, J.(1979). On frictional contact in crack analysis. *Engineering Fracture Mechanics* **12**, 117-123.

Cordes, R.D. and Joseeph, P.F.(1994). Crack surface contact and internal cracks in a plate with residual stresses. *International Journal of Fracture* **66**, 1-17.

Fredriksson, B.(1976). Finite element solution of surface non-linearities in structural mechanics with special emphasis to contact and fracture mechanics problems. *Computer & Structures* **6**, 281-290.

Klarbring, A.(1986). A mathematical programming approach to three-dimensional contact problems with friction. *Computer Methods in Applied Mechanics and Engineering* **58**,175-200.

Lemke,C.E.(1965). Bimatrix game equilibrium points and mathematical programming. *Management Science* **11**,681-689.

Leung, A.Y.T. ,Chen, G.Q. ,Chen, W.J. (1998). Smoothing Newton method for solving two- and three-dimensional frictional contact problems. *International Journal for Numerical Methods in Engineering* **41**(6), 1001-1027

Liu, S.B. and Tan, C.L.(1992). Two-dimensional boundary element contact mechanics analysis of angled crack problems. *Engineering Fracture Mechanics* **42**(2), 273-288.

Melville, P.H.(1977). Fracture mechanics of brittle materials in compression. *International Journal of fracture* **13**, R532-534.

Murakami Y. (1987). *Stress intensity factors handbook*. Oxford, Pergaman.

Okamoto, N. and Nakazawa, M.(1979). Finite element incremental contact analysis with various frictional conditions. *International Journal For Numerical Methods in Engineering* **14**, 337-357.

Owen D.R.J., Fawkes A.J. (1983). *Engineering Fracture Mechanics: Numerical Methods And Applications*. Pineridge Press Limited, Swansea, U.K.

Reklaitis GV, Ravindran A, Mragsdell K.(1983). *Engineering optimization, Method & Application*. John Wiley and Sons, NY.

Thiagarajan, S. and Alwar, R.S.(1986). Influence of crack closure in the case of an angled crack. *Engineering Fracture Mechanics* **24**, 533-537.

Tsung-Chieh Chen and Wen-Hwa Chen(1998). Frictional contact analysis of multiple cracks by incremental displacement and resultant traction boundary integral equations. *Engineering Analysis with Boundary Elements* **21**, 339-348.

Woo, C.W. , Cheung, Y.K. , Chen, Y.Z. and Wang, Y.H.(1988). A simple model for the contact problem of a finite cracked plate in bending. *Engineering Fracture Mechanics* **29**, 227-231.

Zhong, W.X. and Sun, S.M.(1989). A parametric quadratic programming approach to elastic contact problems with friction . *Computer & Structure* **32**(1),37-43.

Zhong, W.X. and Zhang, H.W.(1997). *Parametric variational principles and its application in engineering* (in Chinese). Science Press, BeiJing.

**Figures**

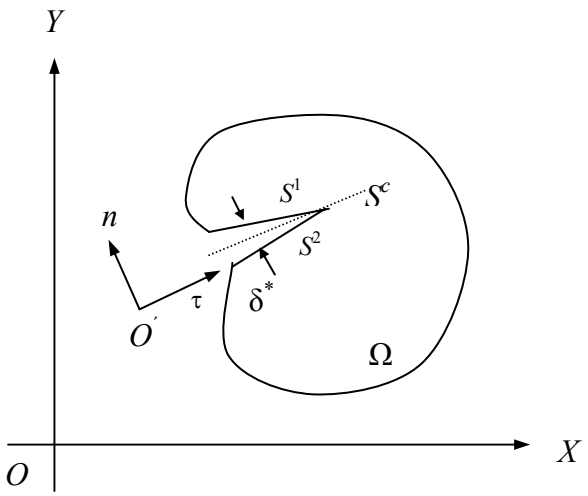


Figure 1. A body with crack of contact faces

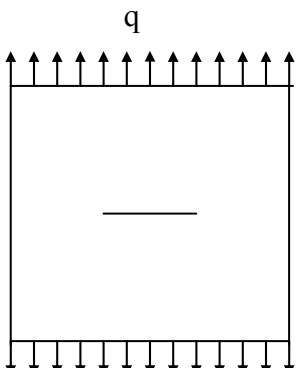

Figure 2. a crack in a field of tensile  tractions

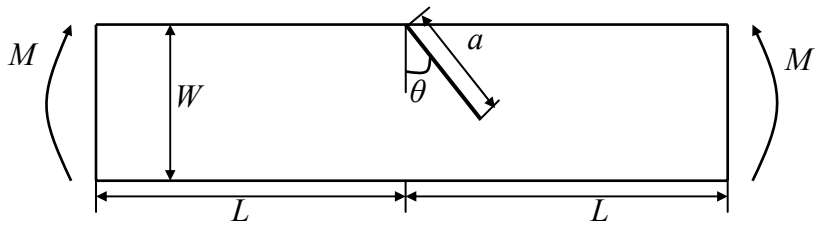


Figure 3. A plate with an angled edge crack under bending

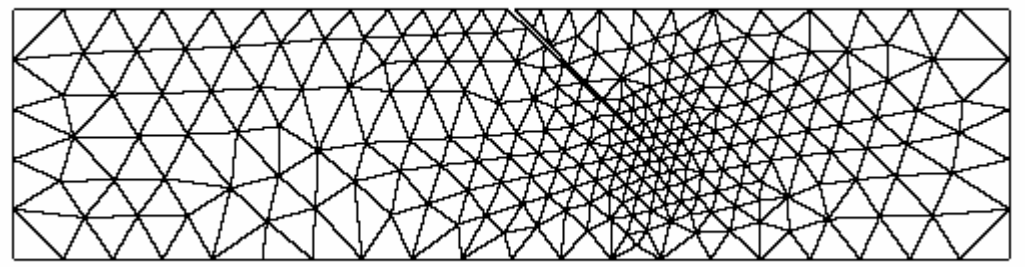

Figure 4. The mesh of plate with edge crack

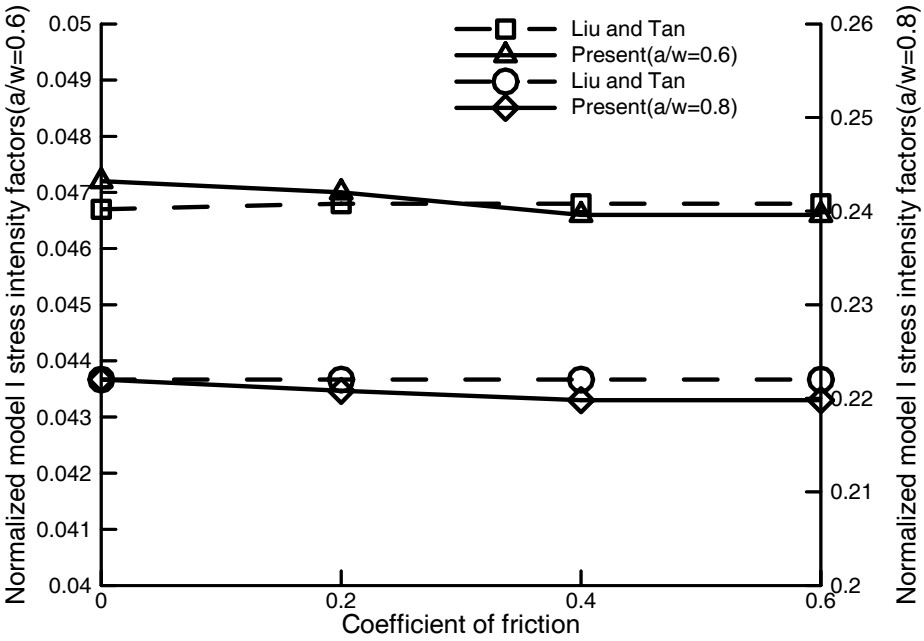


Figure 5. Variation of $K_1^n$ versus the friction coefficient with $\theta=0^0$

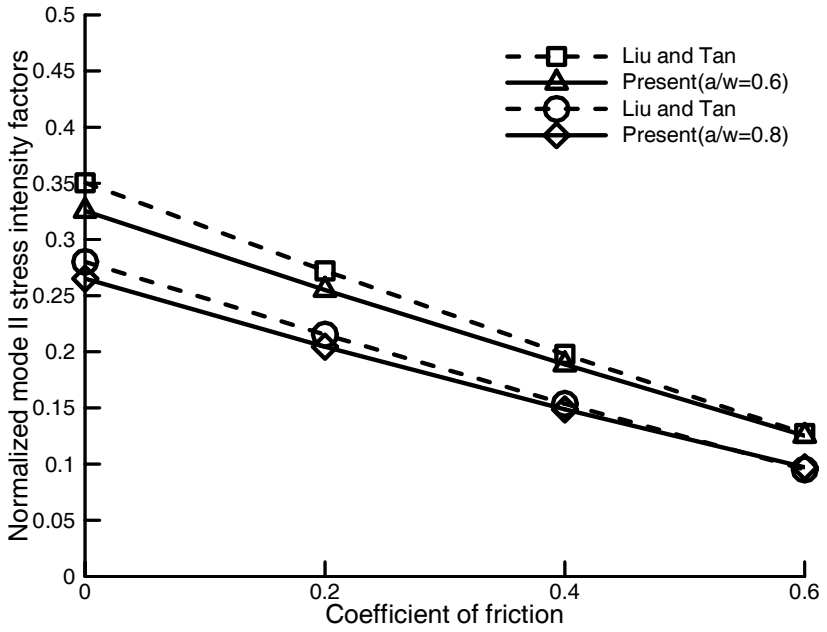


Figure 6. Variation of $K_2^n$ versus the friction coefficient with $\theta=45^0$

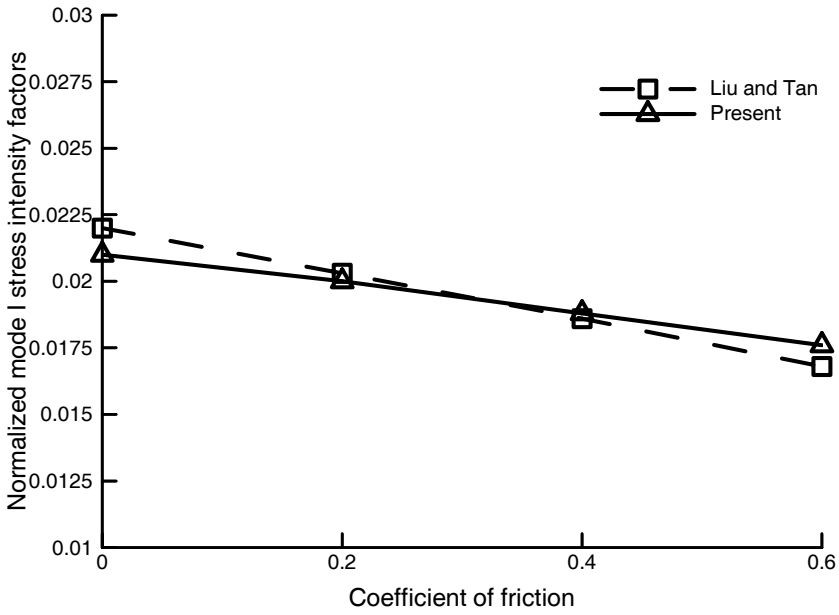


Figure 7. Variation of $K_I^n$ versus the friction coefficient with $\theta=45^0$, a/w=0.8